

Relation between stress field changes and fluid injection at The Geysers Geothermal Field, California: first results

Patricia Martínez - Garzón¹, Marco Bohnhoff^{1, 2}, Grzegorz Kwiatek¹

⁽¹⁾ Helmholtz - Centre Potsdam, GFZ German Research Centre for Geosciences, Potsdam, Germany.

⁽²⁾ Free University Berlin, Institute of Geological Sciences, Berlin, Germany.

Contact: patricia@gfz-potsdam.de

1 Introduction and Motivation

- Potential spatio-temporal variations of the crustal stress field caused by massive fluid injection are important towards an improved understanding of the geomechanical processes involved. However, an accurate and reliable determination of such stress changes based on induced seismicity requires extensive and reliable seismic data.
- We aim at determining potential spatial and/or temporal variations of the local stress field orientation related to fluid injection and extraction at The Geysers Geothermal Field by using two different stress inversion (SI) methods (Table 1).
- Here, we present first results of the SIs performed for a selected cluster of induced seismicity. We also estimate the stress changes before and after the occurrence of a larger magnitude event (LME). We compare the results and reliability of both SIs to results obtained by *Oppenheimer (1986)* for the local stress field in the investigated area.

	SATSI (Hardebeck & Michael, 2006)	MOTSI (Abers & Gephart, 2001)
Input data	Focal mechanisms	First motion data (polarities)
Inversion parameters	Damping parameter, fraction of correctly picked nodal planes	Probability of polarity picked correctly, initial plunge and trend for σ_1 and σ_3
Inversion method	Linearized least square inversion	Non-linear grid search
Output parameters	Orientation of the principal stresses and relative stress magnitude	
	$\varphi = R = \frac{\sigma_2 - \sigma_1}{\sigma_3 - \sigma_1}$	
Uncertainties	Bootstrap resampling	Bayesian
Analysis of subsets	Possibility of inverting stress field for each specified spatio-temporal grid	Inversion for separate regions must be performed outside the program

TABLE 1 : Comparison of SI methods

2 The Geysers Geothermal Field, California

- Induced seismicity associated with the geothermal exploitation at The Geysers (TG) has been extensively monitored for more than 30 years. Since 2007, more than 16500 seismic events with $M > 1$ and 87 events with $M > 3$ have been detected and located within the geothermal area.

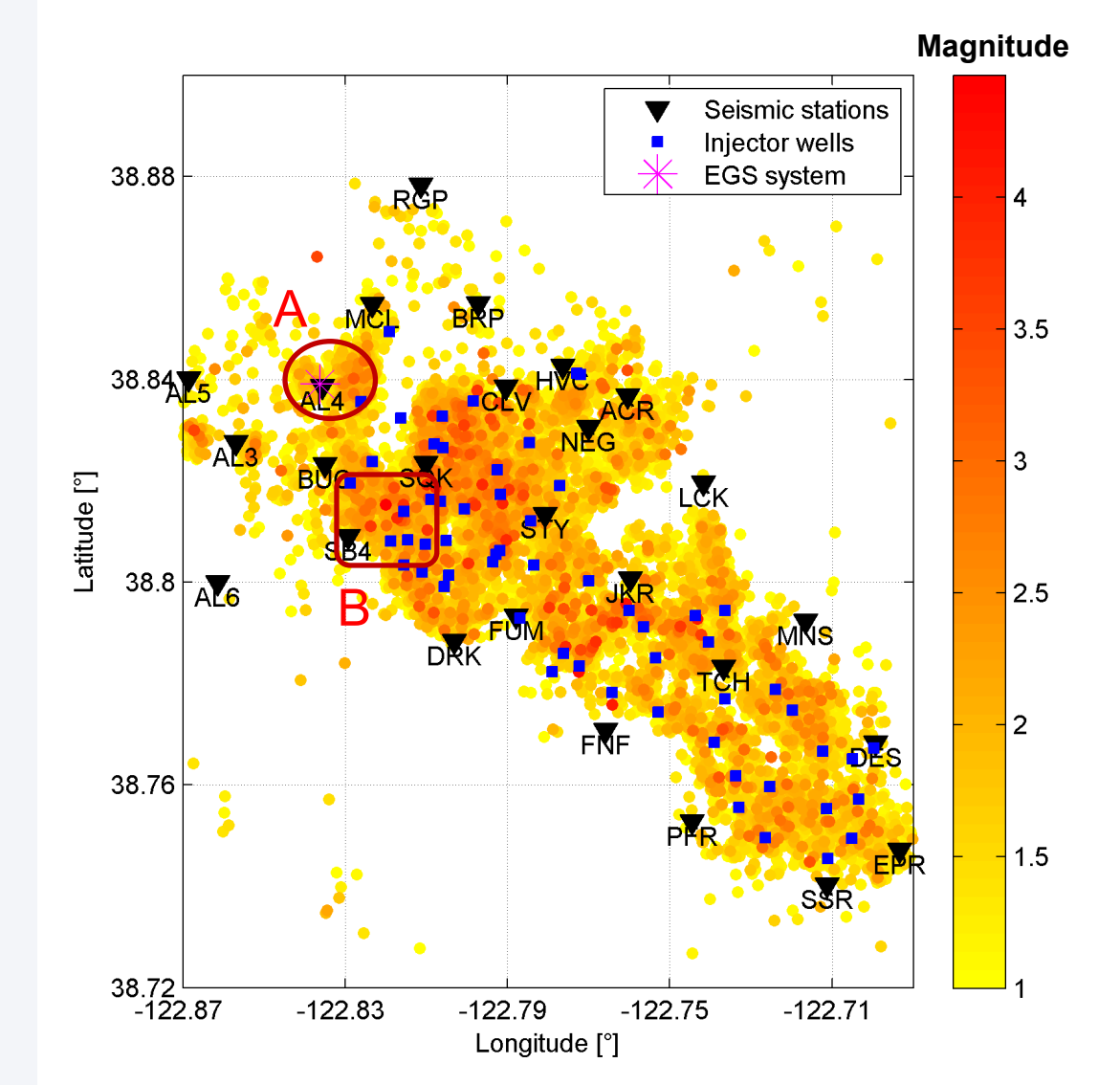


FIG. 1 : Seismicity at TG ($M > 1$) between 2007 and 2012. Magnitude is shown color encoded

Lawrence Berkeley National Laboratory network (LBNL):

- 34 three component surface stations
- Sampling frequency = 500 Hz

Induced seismicity subsets:

- Subset A: Cluster of seismicity related to EGS experiment. $N = 589$ events (August 2007 - July 2011)
- Subset B: Cluster of seismic events before and after occurrence of a larger magnitude event (LME) of $M_w = 4.5$. Events occur within a maximum radius of ≈ 2 km. $N = 724$

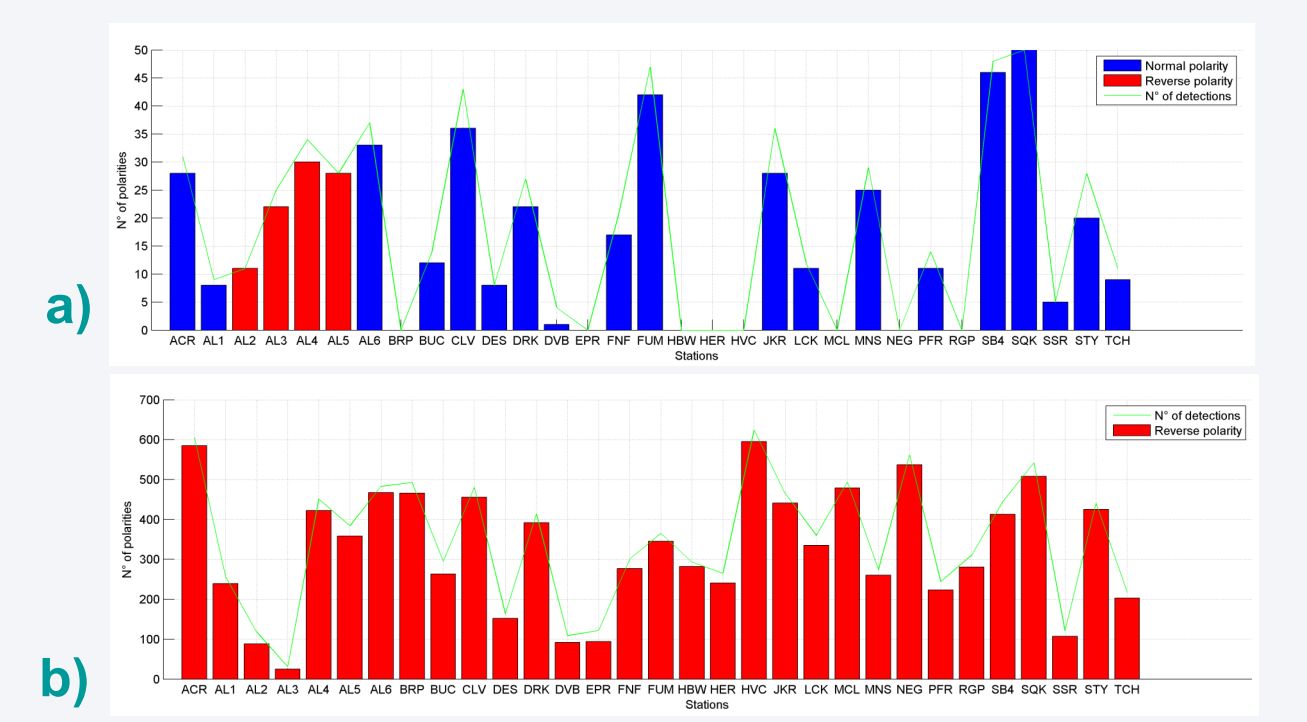


FIG. 2 : N° of polarities detected and picked correctly for each station during a) 6 months of 2008 b) 6 months of 2011

Reliability of picked polarities:

- We investigated the quality of the polarities by comparing them to the expected polarities calculated from available focal mechanisms.
- The original catalog contains data with inappropriate polarities due to different sensor setup.

3 Depth dependence of stress field orientation

- We performed SI for different depth intervals using seismic events of subset A (Fig. 4) which fulfilled defined requirements (minimum of 6 polarities with highest quality of picking).

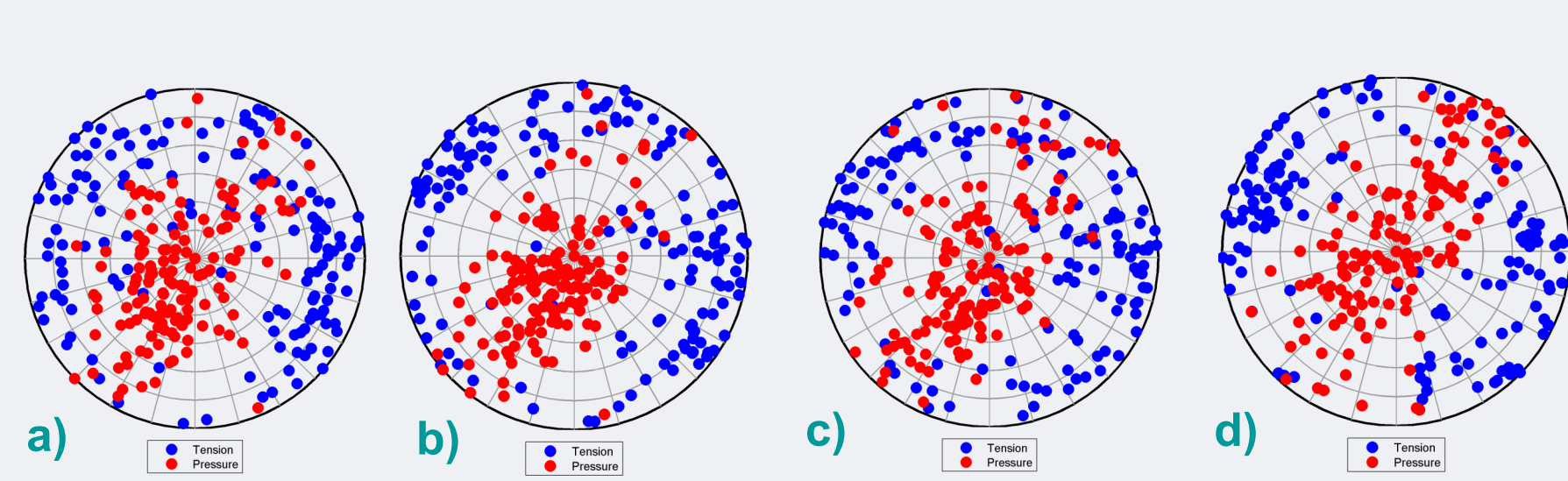


FIG. 3 : Distribution of P and T axes for each depth interval. Average depths: a) 1893 m b) 2300 m c) 2469 m d) 2683 m

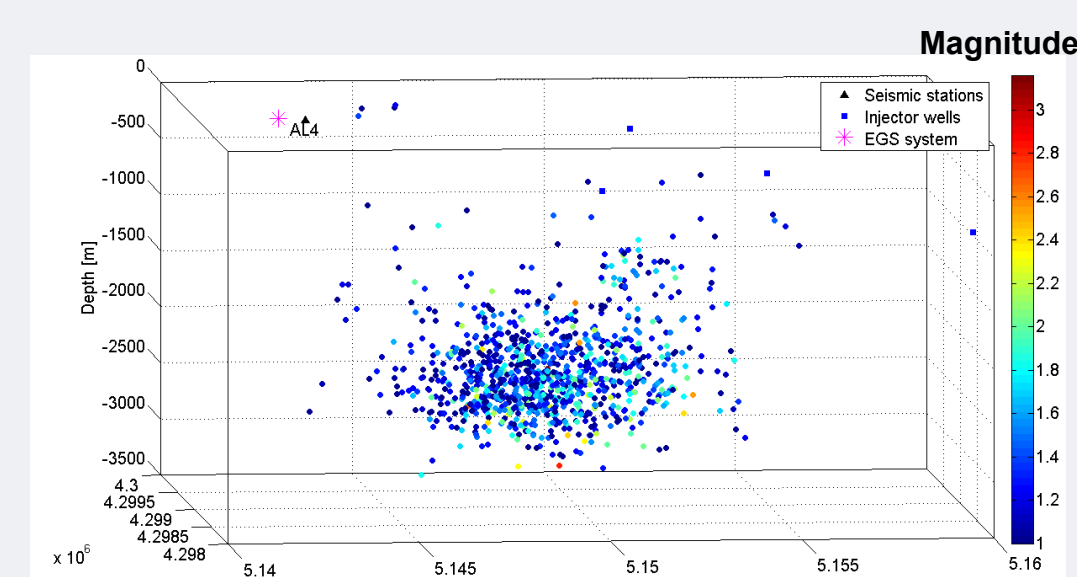


FIG. 4 : Seismic events within subset A. Magnitude is shown color encoded

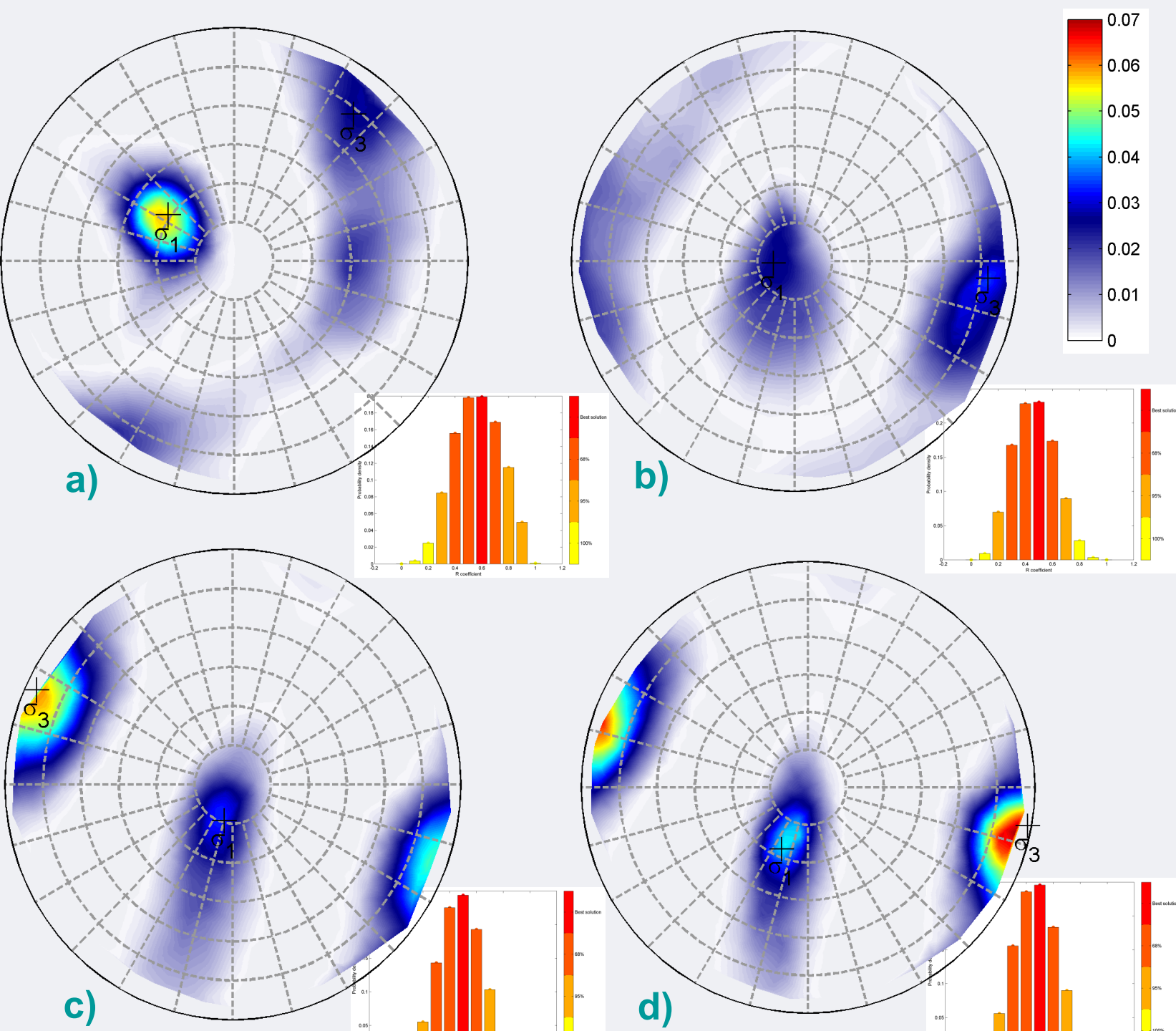


FIG. 5 : Stress axes σ_1 and σ_3 estimated by MOTSI SI together with Bayesian uncertainties. Bottom right part of each plot: distribution of the relative stress magnitude.

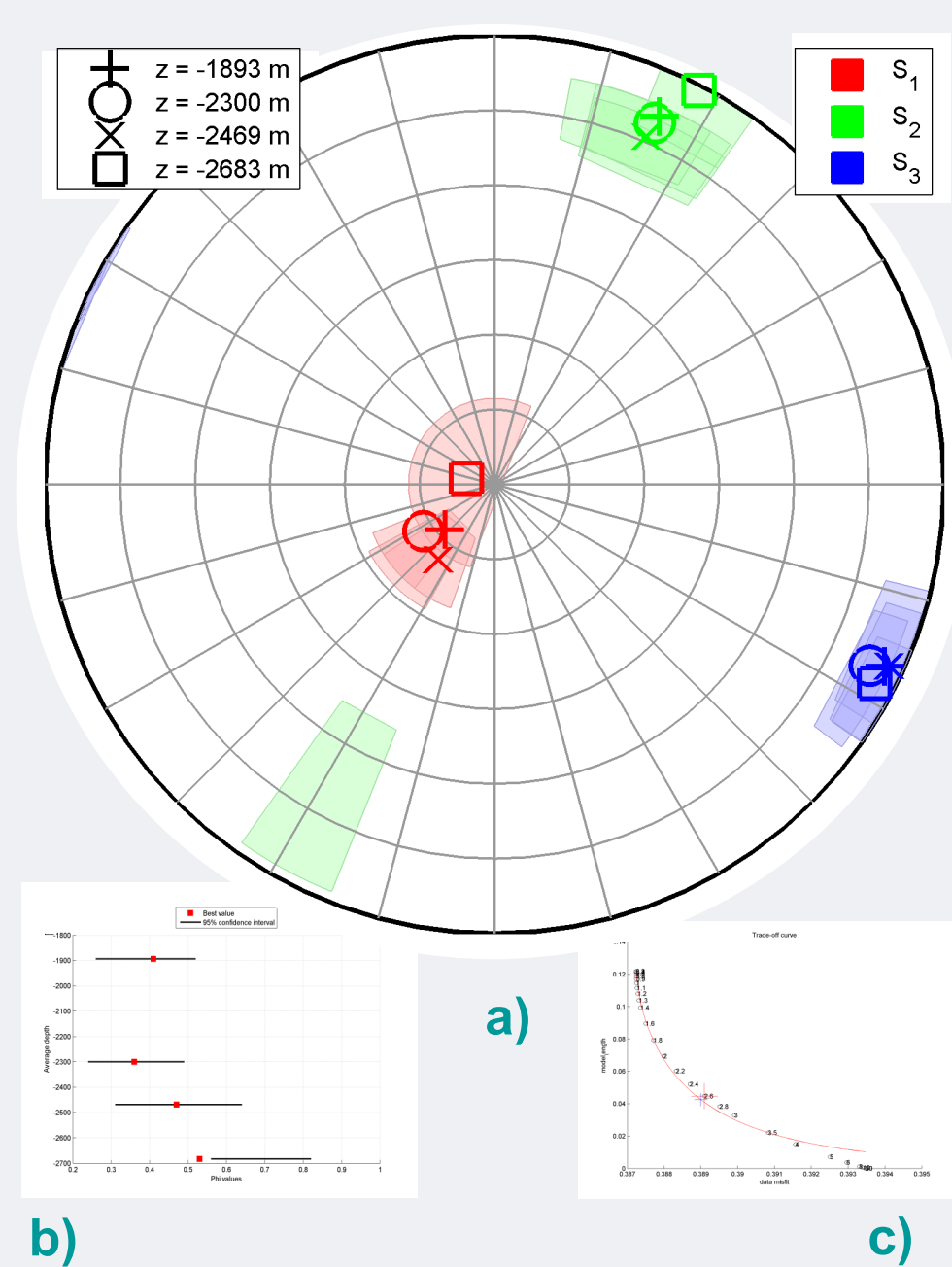


FIG. 6 : a) Principal stress axes estimated by SATSI SI together with 95% confidence intervals b) Relative stress magnitude c) Tradeoff curve

- The results of both inversions indicate a uniaxial extension stress regime with σ_1 being vertical. The small errors obtained with the two different uncertainty assessments demonstrate that the diversity in fault plane solutions is sufficiently high to obtain a reliable result. The results are in good agreement with results of *Oppenheimer (1986)*. However, he obtained that σ_1 and σ_2 have approximately the same magnitude, while we find a value of ≈ 0.5 for the relative stress magnitude, i.e. σ_1 has significantly higher value than σ_2 .

4 Stress changes due to larger magnitude events ?

- We searched for potential stress direction variations associated with LME using the seismic events of subset B (Fig. 8) which fulfill defined requirements.
- Estimation of the appropriate temporal window for the aftershocks was performed by plotting cumulative sum of events (Fig. 7).
- We compared the orientation of the stress field between background seismicity prior/after the LME with the seismicity related to the aftershock sequence.

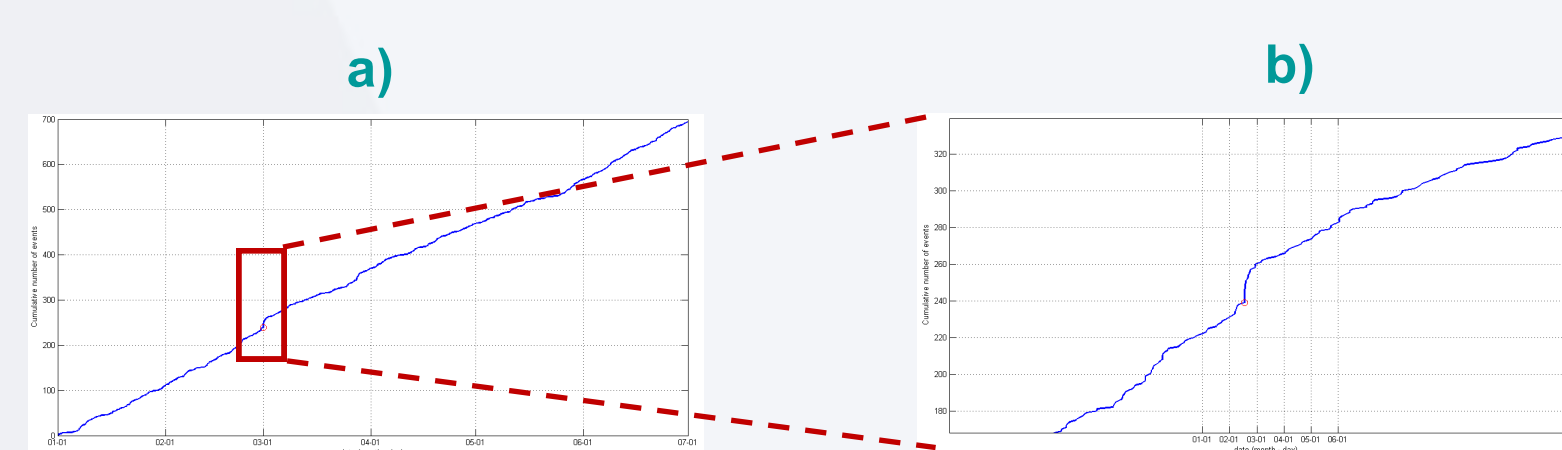


FIG. 7 : Cumulative sum of events during a) the whole time interval of subset B b) Some days before and after LME.

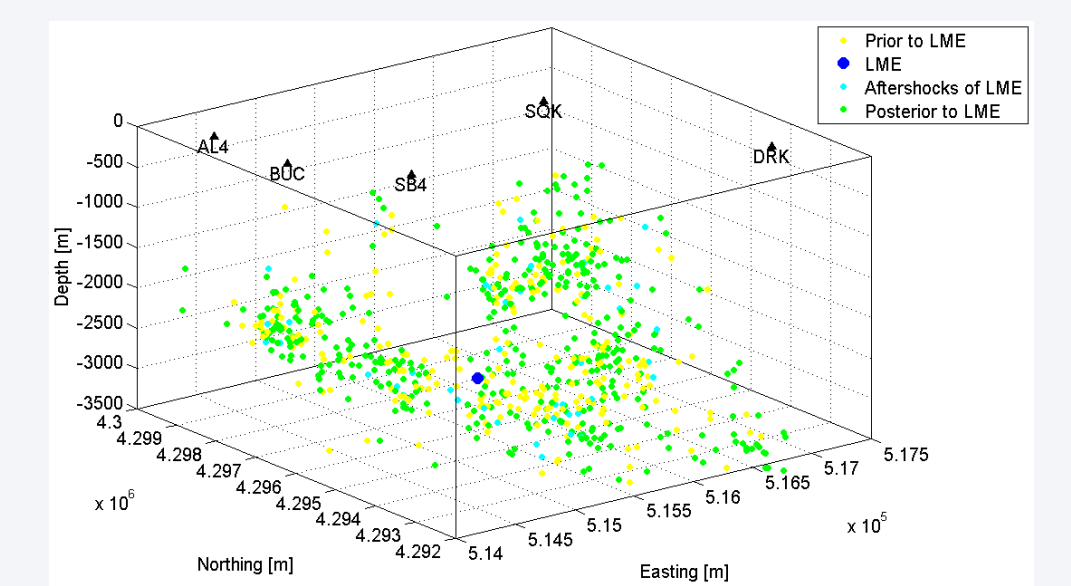


FIG. 8 : 3 - Dimensional plot of the seismic events of subset B

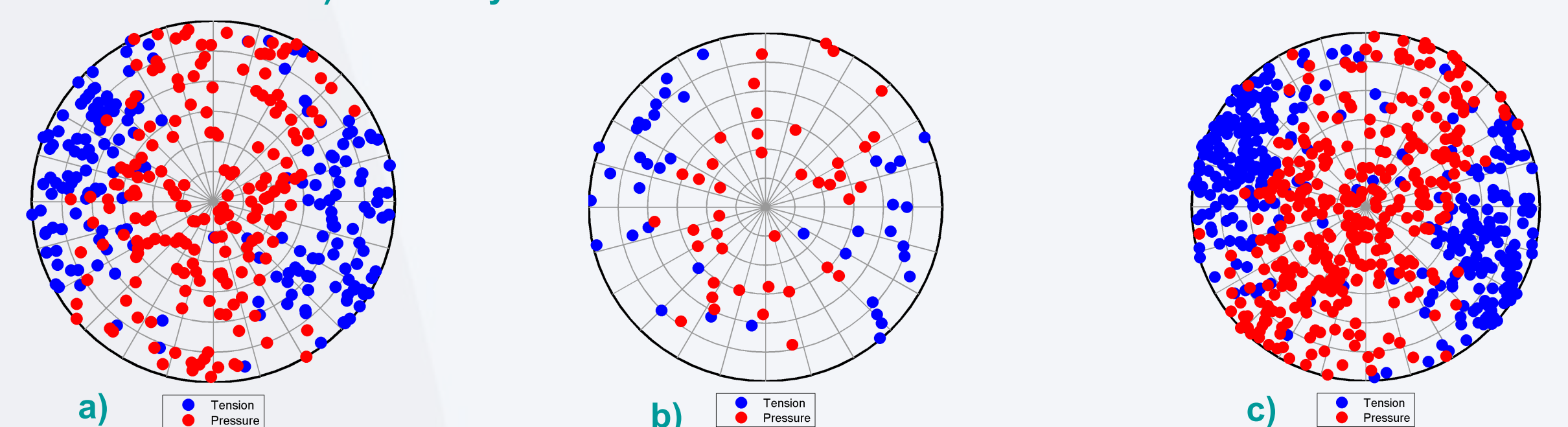


FIG. 9 : Distribution of P and T axes for each time interval. a) Before LME b) LME and aftershock distribution c) Posterior seismicity.

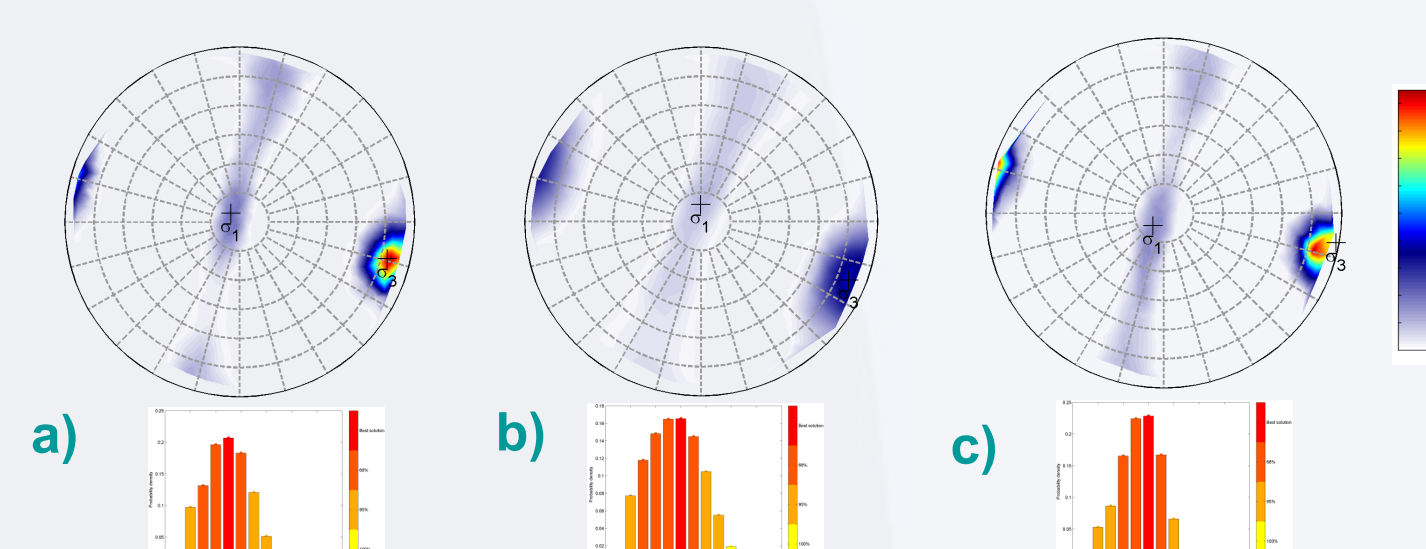


FIG. 10 : Principal stress axes estimated by MOTSI SI. Bottom plot: estimated R. a) Before LME b) LME and aftershock distribution c) Posterior seismicity.

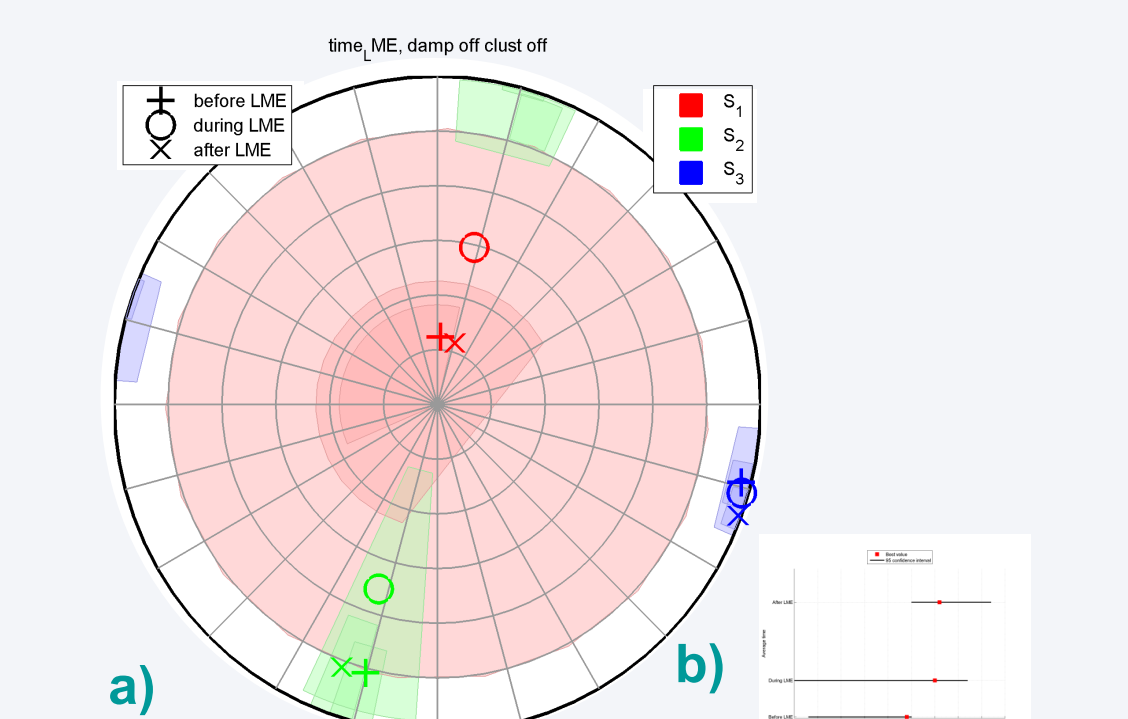


FIG. 11 : a) Principal stress axes estimated by SATSI SI. b) Relative stress magnitude

- P - T plots suggest that during the aftershock sequence the direction of the P axis varies in both trend ($\approx 15^\circ$) and plunge towards more strike slip regime.
- The results of MOTSI SI present relatively small variations of σ_1 and σ_3 . However SATSI SI displays a change in the direction of stress field during the aftershock sequence following LME.

5 Conclusions

- Due to the high rate of seismicity at The Geysers Geothermal Field, the study provides a good opportunity to have a better understanding of the effects of long term fluid injection on the geomechanical state of the reservoir.
- First results of stress inversion in a seismic cluster located below an EGS site indicates that the local stress regime is normal faulting, with σ_3 nearly horizontal with a trend of approximately 105° . No significant change of stress orientation with depth was detected.
- The time dependent stress inversion for the data including the larger magnitude event ($M_w = 4.5$) suggests that it introduced a temporary stress reorientation. However, uncertainties should be recalculated to obtain a more reliable result.
- This study will be continued to further investigate potential stress field changes at The Geysers related to massive fluid injection.

Acknowledgements

- We acknowledge Northern California Earthquake Data Center (NCEDC) for making the data available to be used, Geoffrey A. Abers for releasing MOTSI stress inversion code, Roland Gritto for his help regarding seismic network setup at TG and database, Dough Neuhauser and David H. Oppenheimer for their useful answers to some questions, and Michele Ickrath for fruitful discussions.

References

- Abers, G. A. and Gephart, J. W. (2001). Direct inversion of earthquake first motions for both the stress tensor and focal mechanisms and application to southern California. *J. Geophys. Res.* 106, 26523-26540.
- Hardebeck, J. L. and A. J. Michael (2006). Damped regional-scale stress inversions: Methodology and examples for southern California and the Coalinga aftershock sequence. *J. Geophys. Res.*, 111, B11310.
- Oppenheimer, David H. (1986). Extensional tectonics at The Geysers geothermal area, California. *J. Geophys. Res.* 91, 11463-11476.